

## High sensitive optical microelectronics sensors for the control of pollutants

F. Prieto<sup>1</sup>, L.M. Lechuga<sup>1</sup>, A. Calle<sup>1</sup> & C. Domínguez<sup>2</sup>

*Centro Nacional de Microelectrónica (CNM-CSIC)*

<sup>1</sup>*IMM. Isaac Newton, 8 - 28760 Tres Cantos, Madrid (Spain)*

<sup>2</sup>*IMB. Campus UAB - 08193 Bellaterra, Barcelona (Spain)*

*E-Mail: cnmar03@fresno.csic.es*

### Abstract

The determination of organic contaminants is done, nowadays, mostly by laboratory-based analytical techniques. This analytical methodology involves multistep time-consuming preparation procedures together with expensive and sophisticated techniques, that even leave unsolved problems (i.e. polar and non-volatile degradation compounds). Although the development of immunochemical kits, a few years ago, improved the performance of the result in the environment control, there is still a clear requirement for the development of sensors of small size, reliable, sensitive and selective, which can be operated in-situ and on-line and can be produced by a low cost technology. For that reason, a great interest has focused on the development of selective sensors to control the pollutant processes.

We propose to use an Immunosensor Technology with enhanced specificity and selectivity for the detection of organic contaminants. An immunosensor is a type of affinity sensor comprising antibodies molecules coupled to a transducer, which detects the binding of the complementary analyte to the antibody. The aim of this work is to develop evanescent wave immunosensors based on "ARROW" (*Anti Resonant Reflecting Optical Waveguides*) structures as optimized transducers. The change of the characteristics of the light travelling in the sensor is a measurement of the interaction between the contaminant to be determined and its complementary antibody. The sensors have a Mach-Zehnder interferometric configuration and are fabricated with standard Silicon microelectronics technology. They have dimensions of microns that are compatible with mass-production. After the optimization of the sensor we are going to use them for the monitoring of pesticides (atrazine), phenolic compounds and Irgarol 1051, through the immobilization of their complementary antibody (previously obtained) onto the surface of the waveguide sensor.



## 1 Evanescent wave optical immunosensors

The determination of organic contaminants is done, nowadays, mostly by laboratory-based techniques. However, this methodology requires expensive instrumentation, is time consuming, it can be laborious and it demands skilled personnel. The use of immunological techniques as immunochemical determinations or immunosensors for the measurement of environmental pollutants, is characterized by its simplicity, sensitivity and low cost. Moreover, antibodies can be prepared against virtually any contaminant molecule.

Immunosensors have basically two principal components: a receptor layer and a transducer (Turner[1], Vo-Dinh[2]). The receptor layer has to be capable of specifically recognize the desired analyte in the presence of other molecules. As a consequence of this recognition, a chemical or physical change will occur in the receptor layer. This layer is immobilized to the transducer device, whose function is to transform the chemical or the physical change into an electrical or optical signal.

Among the different types of physical transducers, those based on optical principles have important advantages respect to other types of transducer systems (i.e., amperometric, potentiometric, acoustic). The most important are their high sensitivity, their freedom from electromagnetic interference, they are non destructive and they can be used in aggressive environments.

Up to now, the most developed optical transducer have been based on fiber optics due to their low cost, small size and flexible geometry (Wolfbeis[3]). But the optical fiber can not be designed for a specific application, having to adapt to the telecommunications market offering. Optical fibers also suffer from fragility, especially when they are used as evanescent wave sensors, due to the need of removing the cladding.

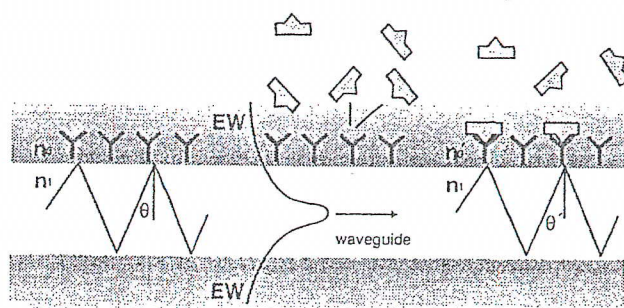


Figure 1. Evanescent wave optical immunosensor.



All these drawbacks have increase the attention to the integrated optical waveguides. In addition to the advantages of using planar waveguides (higher sensitivity, easier deposition of the receptor layer, mechanical stability) the use of microelectronics technology to the design and fabrication of optical waveguides has introduced the advantages inherent to this technology, as miniaturization and mass-production.

In this work, we have developed an evanescent wave immunosensor combining a receptor layer of antibodies together with an integrated optical transducer (Kooyman[4], Lechuga[5]). The detection principle of this transducer makes use of the particular way that optical waveguides transmit light. Although light is confined inside the waveguide, there is a part of it (evanescent field) that travels through a region that extends outward, around a hundred of nanometers, into the medium surrounding the waveguide (see Figure 1). In this type of biosensors, the receptor layer is immobilized onto the waveguide. The biochemical reaction that takes place in this layer produces a change in its optical properties that is detected by the evanescent wave. In addition, the evanescent wave decays exponentially as it penetrates the outer medium. Therefore, it only detects those changes that take place on the surface of the waveguide.

The optical waveguides are based on ARROW (AntiResonant Reflecting Optical Waveguide) structure (Duguay[6], Bartolomé[7]) and the sensor has a Mach-Zehnder interferometric configuration (Schipper[8], Jiménez[9]). A schematic of this sensor is shown in Figure 2. The optical waveguide is split into two arms and after a certain distance they are recombined again. The receptor layer is immobilized to one of the arms (sensor arm) and the other is taken as a reference arm. Light that travels through both arms is compared at the output of the interferometer to analyze the immunological reaction. The advantage of this interferometric configuration is that it presents the lower known detection limit in a direct determination of antibody/analyte pair ( $10^{-12}$ M).

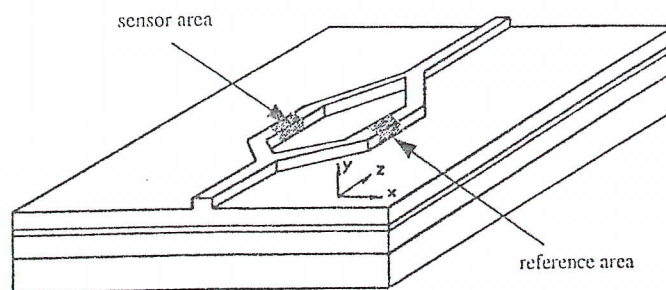


Figure 2. Mach-Zehnder interferometer.



## 2 Fabrication and optical characterization of the structures

### 2.1 Fabrication in clean room

ARROW structures are fabricated using a CMOS compatible process (Moreno[10]). The general structure (Figure 3) is a substrate of Si, a 2  $\mu\text{m}$   $\text{SiO}_2$  first cladding layer of refractive index 1.46, made by thermal oxidation of the Silicon substrate, a 0.3  $\mu\text{m}$   $\text{Si}_3\text{N}_4$  second cladding layer of refractive index 2.00, deposited using Low Pressure Chemical Vapor Deposition (LPCVD) at 800  $^\circ\text{C}$  and a 4  $\mu\text{m}$   $\text{SiO}_x$  core, with refractive index ranging from 1.46-1.48 (depending on x), deposited by Plasma Enhanced Chemical Vapor Deposition (PECVD) at 300  $^\circ\text{C}$ . Rib walls, with a depth of 2.5  $\mu\text{m}$ , are performed by dry Reactive Ion Etching (RIE), where  $\text{CHF}_3$  is used as the etching gas precursor.

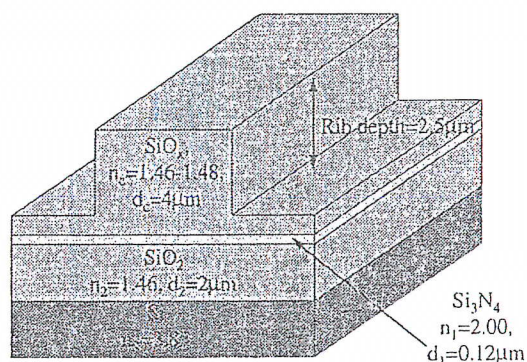


Figure 3. ARROW structure.

For the fabrication of the interferometer, several Mach-Zehnder configurations were designed varying the separation between arms and the Y-junction parameters (angles between branches and Y-junction shape function). On the top of the interferometer, a protective Silicon Nitride layer of 0.12  $\mu\text{m}$  was deposited. Finally, the structure was covered with a silicon oxide layer of 2  $\mu\text{m}$ . In one of the arms, an area of 100  $\mu\text{m}$  wide and 4 or 6 mm large was etched, removing the  $\text{SiO}_2$  layer by wet etching. This zone is the sensor area where the receptor layer will be immobilized. The total length of the Mach-Zehnder interferometer is, for all the samples, of 35 mm. Finally, the sensors are cut in individual pieces and polished for light coupling.



## 2.2 Optical set-up

A schematic of the experimental set-up used is shown in Figure 4. Light from a He-Ne laser ( $\lambda = 632.8$  nm) is coupled to a single mode optical fiber ( $3.8 \mu\text{m}$  core diameter) using a microscope objective (40x). The end of the monomode fiber is placed in front of the waveguide rib face to couple light in the ARROW structure (end-fire coupling). Light is collected by a multimode standard optical fiber ( $50 \mu\text{m}$  core diameter) connected to a silicon photodiode. Precise translation stages are used for the accurate alignment of all the components. A synchronous detection scheme is used with the aid of a lock-in amplifier and a light chopper. Finally, home made software was available for collecting the measurement data.

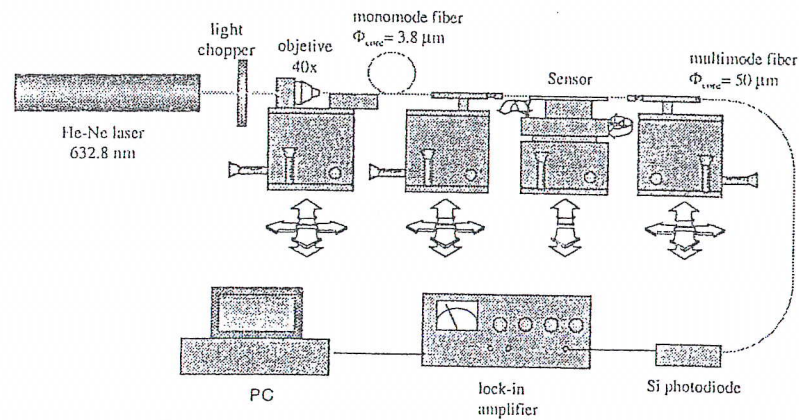


Figure 4. Experimental set-up.

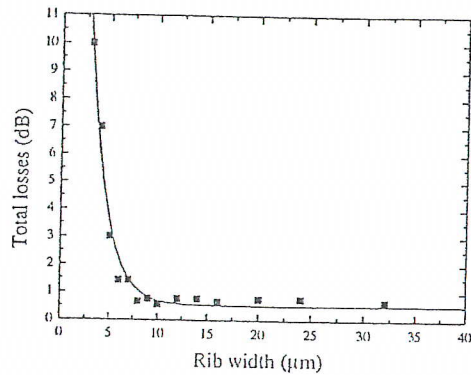
## 2.3 Optical characterization

We analyzed the guiding conditions of the rib-ARROW channel structure measuring attenuation as a function of the rib width, at 632.8 nm wavelength. We had 18 samples with different rib widths, ranging from 1 to 40  $\mu\text{m}$ . Results may be seen in Figure 5(a). Total losses show a very sharp increase for rib widths lower than 10  $\mu\text{m}$ , mainly due to the increase of insertion losses because the optical fiber core diameter is 3.8  $\mu\text{m}$ .

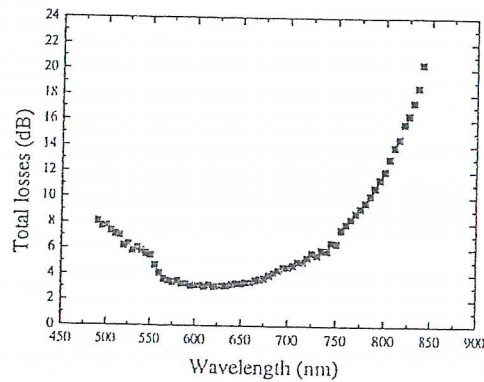
ARROW structure was designed for minimum losses at a wavelength of 632.8 nm. This was verified measuring attenuation as a



function of wavelength using a Hg lamp and a Jobin Yvon-Spex monochromator. Figure 5(b) shows the obtained attenuation for a 1 cm long, 32  $\mu\text{m}$  wide ARROW structure. Minimum losses can be observed around the designed wavelength.



(a)



(b)

Figure 5. Attenuation measurements versus (a) rib width; (b) wavelength.

Finally, modal behaviour of the ARROW structure was investigated by field distribution measurements at the end of the waveguide, using a silicon CCD camera. All the measured waveguides support only one ARROW mode in the transversal direction. However, lateral single mode



behaviour is only found for rib widths lower than 10  $\mu\text{m}$ , as it is shown in Figure 6.

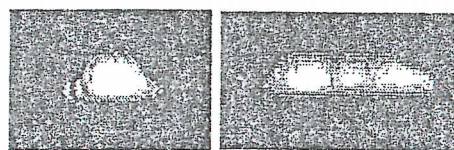


Figure 6. Field distribution for 9  $\mu\text{m}$  and 20  $\mu\text{m}$  wide ARROW s, respectively.

### 3 Sensitivity calculations

To achieve an efficient behaviour of the transducer system, it is necessary to assure a high sensitivity, that is, the sensor response for changes in the optical properties of the receptor layer has to be as high as possible. Sensitivity is evaluated as the changes in the effective refractive index ( $N$ ) for the binding of molecules to the interface between the waveguide and the cover medium (Tiefenthaler[11]). Assuming that the molecules form a homogeneous adlayer of thickness  $d_l$  and refractive index  $n_l$ , the following expression for the surface sensitivity is obtained:

$$\frac{\partial N}{\partial d_l} = \frac{n_c^2 - N^2}{N \cdot d_{eff}} \cdot \frac{n_l^2 - n_o^2}{n_c^2 - n_o^2} \cdot \left[ \frac{\left( \frac{N}{n_o} \right)^2 + \left( \frac{N}{n_l} \right)^2 - 1}{\left( \frac{N}{n_o} \right)^2 + \left( \frac{N}{n_c} \right)^2 - 1} \right]^\rho$$

$$\rho = \begin{cases} 0 & \text{TE mode} \\ 1 & \text{TM mode} \end{cases}$$

where  $n_c$  and  $d_{eff}$  are the refractive index and effective thickness of the core, respectively, and  $n_o$  is the refractive index of the cover medium.

The sensitivity for adsorption of a protein adlayer ( $n_l = 1.45$ ) from an aqueous solution ( $n_o = 1.33$ ) was simulated, as a function of the core thickness  $d_c$ , with the aid of a home-made computer program based on the Finite Difference Method (FDM). For each core value, the optimum ARROW structure was calculated to obtain the corresponding fundamental mode effective refractive index,  $N$ , and effective core thickness,  $d_{eff}$ . Figure 7 shows the results for  $d_c$  ranging from 4  $\mu\text{m}$  to 1  $\mu\text{m}$ . As it may be observed, sensitivity increases as the core thickness



diminishes because the electric field of the guided mode at the interface between the waveguide and the cover medium is stronger, and it is this evanescent field which probes the adsorbed layer.

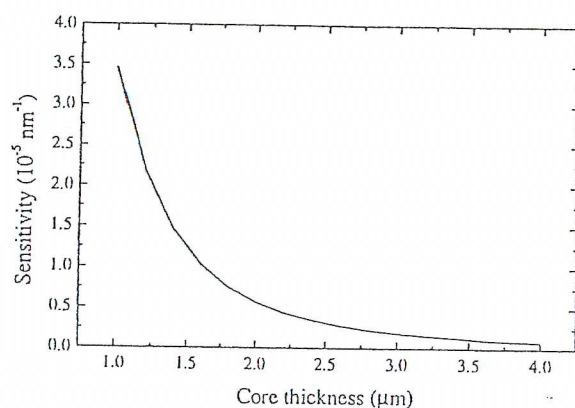


Figure 7. Sensitivity for adsorption of a protein adlayer.

## 4 Preliminary results

Theoretically, waveguides with small core thickness (around a hundred of nanometers) are more interesting because its higher sensitivity. However, this is not so appropriate from a technological point of view. To come to an agreement, we have decided to fabricate sensors with core thickness of 4, 3 and 1.5  $\mu\text{m}$ . On the other hand, the surface sensitivity can be also increased by an appropriate chemical modification of the sensor surface inside the evanescent region. It is out of the scope of this article to study that subject.

Preliminary results of the integrated Mach-Zehnder interferometer used as a differential refractometer (i.e., for measurements of refractive index changes of the cover medium) have been performed. The waveguide has a core thickness of 4  $\mu\text{m}$ , therefore we expect to have a low sensitivity.

The sensor area was covered with a glucose solution of different concentrations, so the refractive index was varying from 1.34 to 1.45. Figure 8 shows the intensity variation at the interferometer output as a result of the refractive index changes. Measurements with the other interferometers are still in progress and we expect to obtain more sensitive results. Measurements with the pollutants are also in progress.



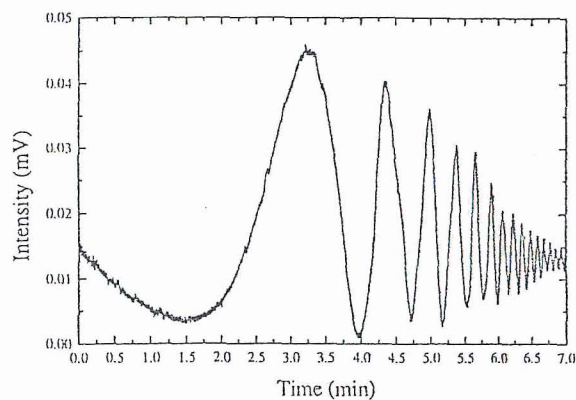


Figure 8. Intensity variation of the interferometer output after the introduction of a glucose solution.

## 5 Conclusions

In this work we have designed and fabricate an integrated Mach-Zehnder interferometer for immunosensing applications. It is based on an ARROW structure ( $\text{Si}/\text{SiO}_2/\text{Si}_3\text{N}_4/\text{SiO}_x$ ), compatible with the Silicon processing Technology. Sensitivity simulations of the ARROW structure show a high surface sensitivity as the core thickness of the waveguide diminishes. As from a technological point of view, core thickness of the order of microns are more interesting, we have decided to fabricate sensors with core thickness as small as  $1.5 \mu\text{m}$ . First measurements of the sensor as a differential refractometer for a  $4 \mu\text{m}$ -thick core are shown. Measurements with the other designed interferometers, as well as with pollutants, are in progress.

## Acknowledgments

The authors would like to thank Andreu Llobera for his valuable help in the numerical simulations. This research has been supported by the CICYT project TIC97-0594-C04.



## References

- [1] Turner, A.P.F., Karube, I., Wilson, G.S. (eds.), *Biosensors: Fundamentals and Applications*, Oxford University Press, Oxford (UK), 1986.
- [2] Vo-Dinh, T., Sepaniak, M., Griffin, G.D. & Alarie, P., *Immunosensors: Principles and Applications*, *ImmunoMethods*, 3, pp. 85-92, 1993.
- [3] Wolfbeis, O.S., *Fiber Optic Chemical Sensors and Biosensors*, CRC Press, Boston, 1991.
- [4] Kooyman, R.P.H. & Lechuga, L.M., Immunosensors based on Total Internal Reflectance, Chapter 8, *Handbook of Biosensors: Medicine, Food and the Environment*, ed. E. Kress-Rogers, CRC Press, Florida (USA), pp. 169-196, 1997.
- [5] Lechuga, L.M., Lenferink, A.T.M., Kooyman, R.P.H. & Greve, J., *Feasibility of Evanescent Wave Interferometer Immunosensors for Direct Detection of Pesticides: Chemical Aspects*, *Sensors and Actuators B*, 24-25, pp. 762, 1995.
- [6] Duguay, M.A., Kokubun, Y. & Koch, T.L., *Antiresonant Reflecting Optical Waveguides in SiO<sub>2</sub>-Si Multilayer Structures*, *Applied Physics Letters*, 22, pp. 892, 1986.
- [7] Bartolomé, E., Moreno, M., Muñoz, J. & Domínguez, C., *Multilayer Analysis of ARROW Structures*, *Microwave and Optical Technology Letters*, 10, pp. 303-307, 1995.
- [8] Schipper, E.F., Brugman, A.M., Domínguez, C., Lechuga, L.M., Kooyman, R.P.H. & Greve, J., *The Realization of an Integrated Mach-Zehnder Waveguide Immunosensor in Silicon Technology*, *Sensors and Actuators B*, 40, pp. 147-153, 1997.
- [9] Jiménez, D., Bartolomé, E., Moreno, M., Muñoz, J. & Domínguez, C., *An Integrated Silicon ARROW Mach-Zehnder Interferometer for Sensing Applications*, *Optics Communications*, 132, pp. 437-441, 1996.
- [10] Moreno, M., Garcés, I., Muñoz, J., Domínguez, C., Calderer, J., Villuendas F. & Pelayo, J., *CMOS Compatible ARROW Guides*, *Proc. of the 8th CIMTEC-World Ceramic Congress and Forum on New Materials*, *Advanced Materials in Optics, Electro-Optics and Communications Technologies*, Firenze (Italy), pp. 465-472, 1995.
- [11] Tiefenthaler, K. & Lukosz, W., *Sensitivity of Grating Couplers as Integrated-Optical Chemical Sensors*, *J. Optical Society of America B*, 6, pp. 209-219, 1989.